

ILSC[®] 2023

Conference Proceedings

This ILSC proceedings paper is made available as pdf-reprint by Seibersdorf Laboratories with permission from the Laser Institute of America.

Third party distribution of the pdf is not permitted.

This ILSC proceedings reprint can be downloaded from
<http://laser-led-lamp-safety.seibersdorf-laboratories.at>

Copyright 2023, Laser Institute of America, Orlando, Florida. The Laser Institute of America disclaims any responsibility or liability resulting from the placement and use in the described manner.

The LIA plans to make the ILSC 2023 proceedings papers available online at a later date.

Reference information for this proceedings paper

K. Schulmeister and P. Rauter

Examples of multiple pulse computer model predictions for laser induced retinal injury thresholds,

International Laser Safety Conference, ILSC 2023, USA, Paper #P102, pages 287-293

Published by the Laser Institute of America, 2023, Orlando, Florida, USA

Please **register** to receive our ***Laser, LED & Lamp Safety* NEWSLETTER**
with information on new downloads, including when this paper has been published:
<http://laser-led-lamp-safety.seibersdorf-laboratories.at/newsletter>

EXAMPLES OF MULTIPLE PULSE COMPUTER MODEL PREDICTIONS FOR LASER INDUCED RETINAL INJURY THRESHOLDS

Paper # P102

Karl Schulmeister and Patrick Rauter

Seibersdorf Laboratories, 2444 Seibersdorf, Austria

Abstract

A validated computer model was used to calculate temperature profiles and predict laser induced retinal injury thresholds for multiple pulses. The data is presented for a wavelength of 530 nm and a pulse duration of 1 ms and for extended sources. Threshold data is presented for varying number of pulses (i.e. varying exposure duration) and pulse repetition frequencies. The threshold data can be presented as average power and as energy per pulse. For high repetition rates, as expected, there is negligible cooling from pulse to pulse and the injury threshold when plotted as average power is equivalent to cw radiation. However, it will be shown that there is an intermediate pulse frequency range with some cooling between pulses, but not completely, so that there is a gradual build-up of background temperature on top of which the heating due to pulses leads to a higher overall temperature increase per pulse. The injury threshold when expressed as energy per pulse decreases with increasing number of pulses. This is the regime where the computer model predictions show that a reduction factor C_P in ANSI Z136.1 and C_5 in IEC 60825-1 less than 1 is needed and the current definitions of this factor are appropriate for the example given. Pulse frequencies less than the critical one have a less pronounced reduction of threshold.

Introduction

In 2014, the third edition of IEC 60825-1 was published [1] as well as a new edition of ANSI Z136.1 [2]. For pulse durations longer than 5 μ s in the wavelength range of 400 nm to 1050 nm and pulse duration longer than 13 μ s in the range of 1050 nm 1400 nm, the rules of how to apply maximum permissible emission limits (MPEs) and accessible emission limits (AELs) for Class 1 to multiple pulses in both documents are equivalent. In this paper, we refer to IEC 60825-1 but the discussion also pertains in the same way to ANSI Z136.1-2014.

The changes of IEC 60825-1 Edition 3.0 with respect to earlier editions were reviewed in an ILSC 2013 paper [3] as well as in a White Paper [4]. Specific issues related to the analysis of multiple pulses and discussed

in 2015 [5] were published in an Interpretation Sheet for IEC 60825-1 Edition 3.0.

The present paper relates to the rules laid down in subclause 4.3 f) of IEC 60825-1 which describe how classification of products with pulsed emission (or scanned emission that leads to a pulsed accessible emission pattern) has to be performed. As in previous editions, three criteria are given that have to be considered in parallel, i.e. it depends on the specific emission pattern which of the three criteria is the most restrictive one that limits the emission of a certain product to remain within a certain safety class (such as Class 1). The present discussion relates to the reduction factor C_5 and therefore to limits that can be associated with retinal thermal hazards (wavelength range of 400 nm to 1400 nm). The three criteria (requirements) that have to be applied can be described as follows:

1) Single pulse criterion

The accessible emission (AE) of each single pulse has to be below the single pulse AEL, where the AEL is determined for the corresponding pulse duration.

2) Average power criterion

The accessible emission expressed as average power (averaged over a certain time period) has to be below the AEL applicable for that averaging duration. For regular emission patterns (constant pulse duration, period and energy per pulse) the critical averaging duration is always equal to T_2 for Class 1 and equal to 0.25 s for Class 2. For irregular emission patterns, the averaging time period has to be varied, i.e. the AE and the AEL are both determined for some averaging time window that is varied both in terms of duration as well as in terms of temporal position within the pulse train. It was shown in reference [5] that the average power rule is equivalent to comparing integrated energy to the AEL expressed as energy; also Criterion 2) can be seen as extension of Criterion 1) when the shortest “averaging duration” used is the duration of a single pulse.

3) Reduced single pulse criterion

Criterion 3) requires the application of C_5 (see rules for determination of C_5 below) to reduce the single pulse AEL, i.e. a more restrictive version of Criterion 1) (or the same for the case where $C_5 = 1$). As a basic rule, C_5

is a function of N and N is the number of pulses within T_2 (or 0.25 s for Class 2). This factor C_5 is applied to reduce the single pulse AEL, and the AE of every single pulse has to be below this reduced AEL. While applying this rule on a regular pulse train is straightforward, for irregular pulse trains there is the added complexity that groups of pulses have to be treated as “effective pulses” (see also Interpretation Sheet ISH1, [6]), and N is then be the number of occurrences of the group within T_2 . The AEL and AE is determined for the group, i.e. the AEL is determined for the group duration and AE is the energy per group. This rule can be seen as an extension of the average power rule when for each averaging duration, the region within the averaging duration is considered as an “effective pulse”, but additionally to just comparing the energy within the group to the AEL applicable for the group duration, that AEL is reduced by the factor C_5 derived from the number of “effective pulses” within T_2 .

While in the current standard wording, for Criterion 3) it is not specifically noted to apply C_5 in case of pulse groups, based on basic biophysical reasoning (particularly if there is negligible cooling between the pulses within the pulse group) it is necessary to apply Criterion 3) not only to individual pulses but also to pulse groups (in ANSI Z136.1-2014 the grouping is specifically included in the wording). The necessity of the application of C_5 to groups of pulses is also expressed in the Interpretation Sheet ISH 1 for IEC 60825-1 Ed. 3.0 [6].

In contrast to earlier editions of IEC 60825-1 as well as ANSI Z136.1, this grouping became necessary for the 2014 editions of the two standards, because in the latest edition, for emission durations longer than T_i , the reduction factor C_5 (C_P in ANSI) is limited to 0.2 (equivalent to only counting a maximum of 625 pulses) for apparent sources larger than α_{\max} and to 0.4 (equivalent to only counting a maximum of 40 pulses) for apparent sources between 5 mrad and α_{\max} . This limitation of the “extent” of the reduction of the AEL by the factor C_5 did not exist in earlier standards and as a consequence, considering individual pulses only (no grouping) and counting the number of individual pulses (compared to the number of pulse groups, the number of the individual pulses is always larger) the resulting C_5 applied to the AEL of individual pulses was always more restrictive as compared to considering a number of neighboring pulses as one effective pulse.

In this paper, we limit the discussion to the regime of emission durations above 5 μ s and the visible wavelength range, where Criterion 3) reads as follows:

$\alpha \leq 5$ mrad: $C_5 = 1$

$\alpha > 5$ mrad: $C_5 = N^{-0.25}$ with following limited reduction factor (equivalent to maximum values of N):

$\alpha \leq \alpha_{\max}$: C_5 not less than 0,4 (maximum N : 40)

$\alpha > \alpha_{\max}$: C_5 not less than 0,2 (maximum N : 625)

$\alpha > 100$ mrad: $C_5 = 1$

Note that the value of α above is not limited by $\alpha_{\max}(t)$ where t is the emission duration analyzed as pulse.

See also our White Paper “Extended Source AEL Analysis of Scanned Laser Emission for IEC 60825-1” (2023) for a discussion on multiple pulse analysis: <https://laser-led-lamp-safety.seibersdorf-laboratories.at/downloads/e-books-white-papers>

In this paper we limit the discussion to regular pulse trains, i.e. to pulse trains with constant pulse duration, pulse frequency and energy per pulse. Injury thresholds for irregular pulse trains were calculated and analyzed in a different project and presented in earlier publications [7,8]. This work on irregular pulse trains was based on the present rules for C_5 presented above (that is, all in the thermal regime, avoiding micro-cavity induced injury), and a special method to determine N , as “partial N ”, was proposed.

Indirectly, these studies have also confirmed the validity of the existing criteria for regular pulse trains, because for regular pulse trains, the proposed “partial N ” is the equal to the number of pulses N within T_2 .

It is evident, but not always considered in discussions that any change of the analysis rules also needs to make sure that they are appropriate for *irregular* pulse trains.

Example of data confirming $N^{-0.25}$

Parameters

We present threshold predictions from a computer model which was validated against all applicable non-human primate experimental injury threshold data in the regime of thermally induced retinal injury [9].

The data presented is a selection of more than 140 000 threshold values, calculated for

- 530 nm and 1060 nm wavelength
- varying retinal image diameters (top-hat profile)
- varying pulse durations
- varying number of pulses (equivalent to varying exposure durations)
- varying pulse repetition frequencies

A more complete presentation of data will be submitted as a peer reviewed paper. Here we limit the discussion to the following:

- Wavelength of 530 nm
- Pulse duration of 1 ms
- Retinal image diameter (top-hat) equal to 408 μ m equivalent to $\alpha = 24$ mrad

The pulse repetition frequency was varied between 2 Hz and 900 Hz, and $N = 1$ to $N = 1000$ pulses were calculated.

Additionally, for 530 nm and $\alpha = 24$ mrad, the continuous wave injury threshold was calculated for varying exposure durations T . We note that for 1 ms pulse duration and rectangular temporal pulse shapes, a frequency of 1000 Hz is the same as a cw emission.

AEL for Class 1

For an emission duration of 1 ms, $\alpha_{\max} = 6.3$ mrad, so that the chosen angular subtense of the apparent source of $\alpha = 24$ mrad is larger than α_{\max} . The AEL is presented as open - field of view, equivalent to the intra-ocular energy, or intra-ocular power that is used to present injury thresholds. Thus, the threshold given as energy per pulse pertains to the energy in the whole retinal image, not just in the part of the image within an angle of acceptance $\gamma = \alpha_{\max} = 6.3$ mrad. For the comparison with the injury thresholds expressed as intra-ocular energy, the AEL for Class 1 also needs to be expressed in the same way, i.e. in terms of permitted energy passing through the 7 mm aperture stop. The respective open - field of view C_6 is therefore (see discussion in reference [10]):

$$C_6^{\text{open}} = \frac{\alpha_{\max}}{\alpha_{\min}} \cdot \frac{\alpha^2}{\alpha_{\max}^2} = \frac{\alpha^2}{\alpha_{\min} \cdot \alpha_{\max}} = \frac{24^2}{1.5 \cdot 6.3} = 60.7$$

Therefore, the AEL for Class 1 presented as “open” for $t = 1$ ms for a single pulse equals 239 μJ . This is the bases for the multiple pulse Criterion 3.

For the average power Criterion 2, the AEL is determined as average power as function of averaging duration T (which for an MPE analysis is the exposure duration). The duration T is derived from the number of pulses N in the pulse train and the pulse frequency. The duration T spans across the beginning of the first pulse and the end of the last pulse in the respective pulse train.

The injury threshold data can be presented in two ways:

- 1) As average power that at the time T (the duration of the pulse train that is used to calculate the threshold) is predicted to result in injury. This can be compared to the average power Criterion 2 AEL(T).
- 2) As energy per pulse where for the last pulse in the considered pulse train (number of pulses N), injury is predicted. This can be compared to the reduced pulse Criterion 3, i.e. to $\text{AEL}(1 \text{ ms}) \cdot C_5$.

For thresholds expressed as average power for a given exposure duration T , the average power is equal to the

total energy within T (the energy of all pulses added up) divided by T .

In this dual presentation, the underlying thresholds for a given number of N and a given frequency are the same, but the dual presentation is the basis for a visual comparison with the two main analysis criteria.

When AEL(t) as function of $t = T$ is presented as average power, the $t^{0.75}$ dependence of the AEL given as energy up to T_2 transforms into a $t^{0.25}$ dependence. However, also α_{\max} depends on t . There is a critical t_{crit} where $\alpha_{\max}(t_{\text{crit}}) = \alpha$:

$$t_{\text{crit}} = \left(\frac{\alpha}{200} \right)^2 = 14.4 \text{ ms}$$

When T for the calculation of the AEL(T) is longer than t_{crit} , $\alpha = 24$ mrad is smaller than $\alpha_{\max}(T)$ and then:

$$C_6 = \alpha / \alpha_{\min}.$$

When T is shorter than t_{crit} , the formula from above for the open C_6 applies. Thus, there is a change of the open-AEL in the T -dependence at t_{crit} where the dependence of $\alpha_{\max}(T)$ on T results for exposure durations T below t_{crit} results in an overall $t^{0.75}$ dependence for the AEL expressed as total intra-ocular power. This can also be seen in the figure in the subsequent subsection.

Presentation as Average Power

Figure 1 shows the calculated injury thresholds expressed as average power, as function of exposure duration T . The pulse repetition frequency f was varied. Also shown is the average power AEL for Class 1 as function of T for $\alpha = 24$ mrad. We see the change in T -dependence as described above for $T = 14.4$ ms.

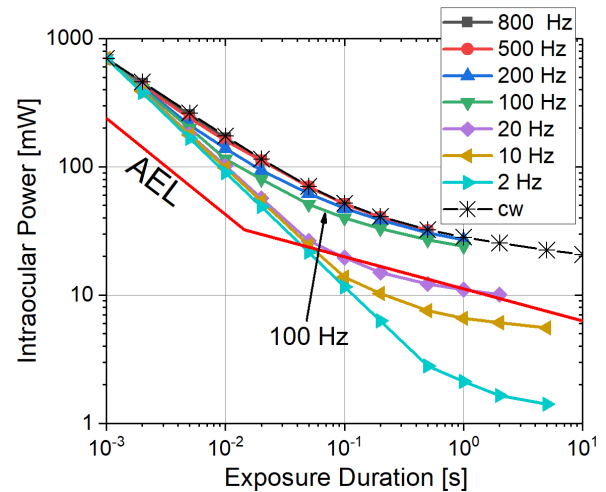


Figure 1. Predicted injury thresholds expressed as average power, for varying pulse frequencies. The AEL for Class 1 as “open” quantity is shown without symbols. The location of the symbols does not depict number of pulses.

We can see that the thresholds for frequency $f = 200$ Hz and higher frequencies are all on top of each other and form the upper bound of the assembly of curves. This is the regime where there is a relatively small degree of cooling between pulses. Correspondingly, in terms of the trend of the thresholds, the exposure can be seen as quasi-cw and the thresholds plotted as average power are equal to the threshold for cw exposure for a given value of T , which is one of the curves of Figure 1. We will see below in Figure 4 that for frequencies equal to 500 Hz and 800 Hz, the temperature increase associated to one pulse when counted from the background temperature is much smaller than the background temperature, for already relatively short exposure durations. The higher the pulse frequency is, the smaller the relative temperature increase per pulse, compared to evolving background temperature becomes.

We can see in Figure 1 that the curve for $f = 100$ Hz is somewhat lower than the “quasi-cw” curves. The next curve for $f = 20$ Hz is even further below the quasi-cw curve and is also somewhat below the respective AEL for Class 1 in the regime between 100 ms and several seconds.

We identify a frequency of about 100 Hz as a critical frequency where the threshold as average power no longer is equivalent to the cw threshold and where the reduction factor (i.e. the safety margin) between the threshold and the average power MPE is reduced.

Presentation as Energy per Pulse

In Figure 2, the same thresholds as above are presented as energy per pulse, referred to as intra-ocular energy. The abscissa in this case is the number of pulses N within the pulse train, so that the predicted thresholds can be compared against the AEL for Criterion 3.

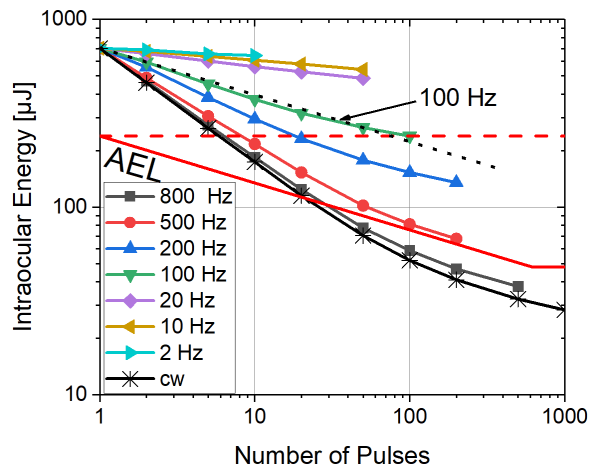


Figure 2. Predicted injury thresholds expressed as energy per pulse, plotted as function of number of pulses N . The AEL for Class 1 is shown without symbols, both for $C_5 = N^{-0.25}$ as well as for $C_5 = 1$.

Figure 2 shows the AEL as function of N as thick solid line, decreasing with $N^{-0.25}$ down to $N = 625$ where $C_5 = 0.2$. As parallel line, the dotted line with the $N^{-0.25}$ trend is shifted to be equal to the threshold for $N = 1$. Also shown as horizontal line is the AEL when there would be no reduction, i.e. for $C_5 = 1$.

We can see that the thresholds expressed as energy per pulse for 100 Hz – which was the “critical” frequency identified from Figure 1 – are basically equal to the trend of $N^{-0.25}$. We will see from the time-temperature curves in the next section that in this frequency regime, there is some cooling until the next pulse starts, but there is still a gradual build-up of the background temperature due to non-complete cooling from pulse to pulse.

For a frequency of 100 Hz, the pulse period equals 10 ms. For 100 Hz, the data was plotted for up to $N = 100$, resulting in an exposure duration of 1,01 s. We see that when C_5 would be equal to $C_5 = 1$ (the horizontal dashed line), the predicted threshold for $N = 100$ would be equal to the AEL for Class 1. Based on ongoing work for larger numbers of N not shown, we see that although the trend of the threshold does not continue with $N^{-0.25}$ but begins to level off. However, it is evident that the threshold will be below the AEL for Class 1 for N exceeding 100 for $C_5 = 1$. Even when one argues with eye movements for exposure durations of 1 second, the safety margin cannot be seen as sufficient for exposure durations shorter than 1 second for the case that $C_5 = 1$.

We see that the thresholds for high frequencies when plotted as energy per pulse lie below the AEL based on Criterion 3. However, this is the regime of quasi-cw thresholds when plotted as average power, where the average power AEL is sufficiently restrictive to overall limit the emission to safe levels. In other words, due to the high frequency, a certain level of average power is reached already for small energy-per-pulse values. Thus, when the thresholds for these high frequencies are plotted as energy per pulse, they are found at low levels. The lowest curve is for a continuous emission. This can be presented in terms of number of pulses considering that one “pulse” (rectangular temporal shape) has a duration of 1 ms and the frequency of 1 kHz results in cw emission. Thus, the cw emission is cut into 1 ms sections with a period of $1/1 \text{ kHz} = 1 \text{ ms}$.

It is interesting to investigate the trend for frequencies smaller than 100 Hz, shown in Figure 2. For the small frequencies, there is more time to cool until the next pulse starts, and for very low frequencies, there is basically complete cooling of the tissue temperature, back to body temperature, before the next pulse starts. Even when there is some residual temperature increase left from the previous pulse, it is small and the build-up of background temperature is slow. In this regime, a constant background temperature is reached after a small number of pulses and from then on, each pulse

then results in the same peak temperature. This means that each pulse also has the same contribution to the damage integral of the model, which, when it reaches a value of unity, is associated to the occurrence of an injury [11]. That is, each pulse results in a fractional injury, or insult to the cell, which for a single pulse does not result in the cell dying. When a sufficient number of pulses is incident on the cell, the insults build up and finally result in cell death (see discussion in reference [11]). For instance, when the pulse train consists of four pulses and there is complete cooling between pulses, each pulse contributes 25% of the damage so that at the end of the last pulse, the cell is sufficiently damaged that it dies. When the pulse train consists of 10 pulses, and injury is induced at the end of the 10th pulse, each pulse contributes 10% partial damage to killing the cell.

We can see in Figure 2 that for low pulse frequencies, the reduction of injury threshold with increasing number of N is small. That is, the curves lie much higher than the $N^{-0.25}$ trend. This low reduction of threshold for increasing N might be puzzling considering that each pulse contributes some partial damage to the cell. When there are more pulses, each needs to contribute correspondingly less partial damage to reach 100%. The answer lies in the strong non-linearity of the dependence of thermal injury on temperature: a small decrease of the temperature in the tissue results in a very strong (exponential) decrease of the damage integral [10]. Therefore, only a small amount of reduction of the temperature is sufficient to compensate for the contribution of larger number of pulses to the overall damage. A small amount of temperature decrease is directly associated to a small reduction in injury threshold as function of N .

Thus, we can see that the stronger reduction of the injury threshold found for the critical frequency of 100 Hz is based on a combination of the individual contribution of the pulses in terms of partial damage, together with the gradual increase of the background temperature due to imperfect cooling. Due to the non-linearity of thermal injury, the increase of the peak temperature due to non-perfect cooling between pulses has a strong effect on the damage integral, i.e. on the effectiveness to induce cell damage. The pulses at the beginning of the pulse train, when the background temperature is still low, contribute to the overall damage only on a small level and it is the pulses later on in the pulse train, that “sit on” the elevated background temperature, that are mostly relevant for inducing the injury. Due to the non-complete cooling from pulse to pulse, the energy needed to result overall in critical temperatures that induce cell death is correspondingly reduced compared to lower frequencies with more pronounced cooling until the next pulse heats the tissue.

Time-Temperature Profile

The discussion in the previous section already noted the background of the dependence of the threshold on the number of pulses, or the exposure duration. In this subsection, we plot the calculated retinal temperature in the center of the 408 μm top-hat profile as function of exposure duration. The parameters are given as above, i.e. 530 nm wavelength and 1 ms pulse duration. The temperatures shown in Figure 3 were calculated with the energy per pulse that for the respective pulse frequency reaches the injury threshold for 100 s exposure duration.

For a given pulse frequency, the temperature increase per pulse when determined from the start-temperature is directly related to the energy per pulse and does not change for increasing exposure duration. We see in Figure 3 that the temperature increase per pulse above background for 100 Hz is significantly less than for 30 Hz and 10 Hz. This is directly associated to the lower injury threshold for 100 Hz when plotted as energy per pulse seen in Figure 2. We can also see for 100 Hz that at the time when the next pulse starts, the temperature increase from the previous pulse has not cooled down and there is a notable increase of the background temperature from pulse to pulse. This effect is much lower for 30 Hz and even more so for 10 Hz.

In Figure 3, the time-temperature profiles were calculated for the respective energy per pulse that for the given pulse frequency is calculated to lead to injury at 100 s of exposure to the pulses. The respective energy-per-pulse values vary considerable for the pulse frequencies shown in Figure 3, which can be seen best based on the temperature increase associated to the first pulse, which is directly related to the energy per pulse. The temperature increase for the first pulse is about 5 K for 100 Hz but almost 20 K for 10 Hz.

It is also instructive to calculate the time-temperature profiles for the energy per pulse being the same for all pulse frequencies, which is shown in Figure 4.

When for all pulse frequencies the energy per pulse is the same (chosen as the threshold energy for one pulse), the effect of the intra-pulse cooling can be seen best. When for high pulse frequencies there is little cooling between the pulses, the background temperature on top of which the heating of the individual pulses “sit” increases drastically with exposure duration.

For 10 Hz and 30 Hz the background temperature increase is correspondingly low.

The critical frequency of 100 Hz can be said to be in a regime where the temperature increase per pulse above background is roughly equal to the background temperature above the starting temperature of 310 K, in the regime after approximately 20 pulses when the background temperature for 100 Hz has reached the steady state, i.e. a constant background temperature.

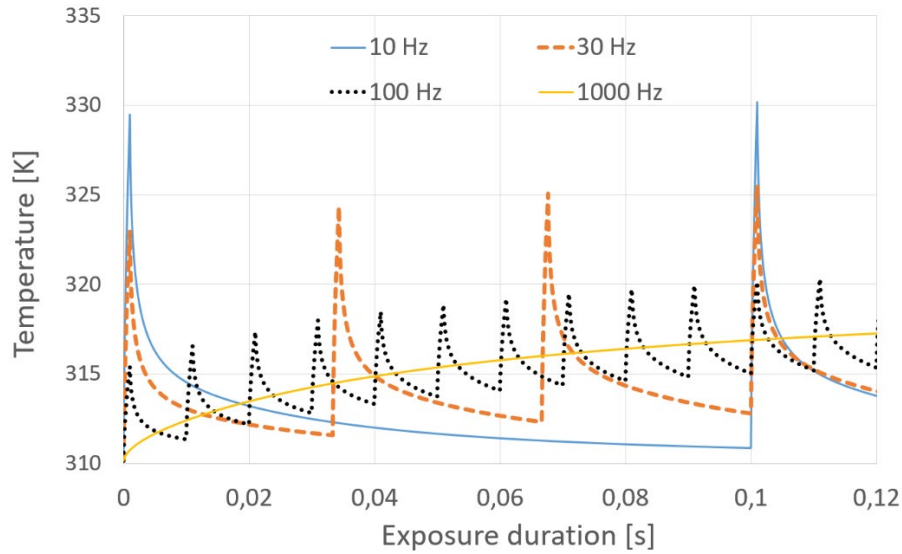


Figure 3. The time-temperature history for pulse frequencies between 10 Hz and 100 Hz, as well as for cw (1000 Hz). The temperature was calculated for the respective energy per pulse that is calculated to lead to injury for 100 s exposure duration.

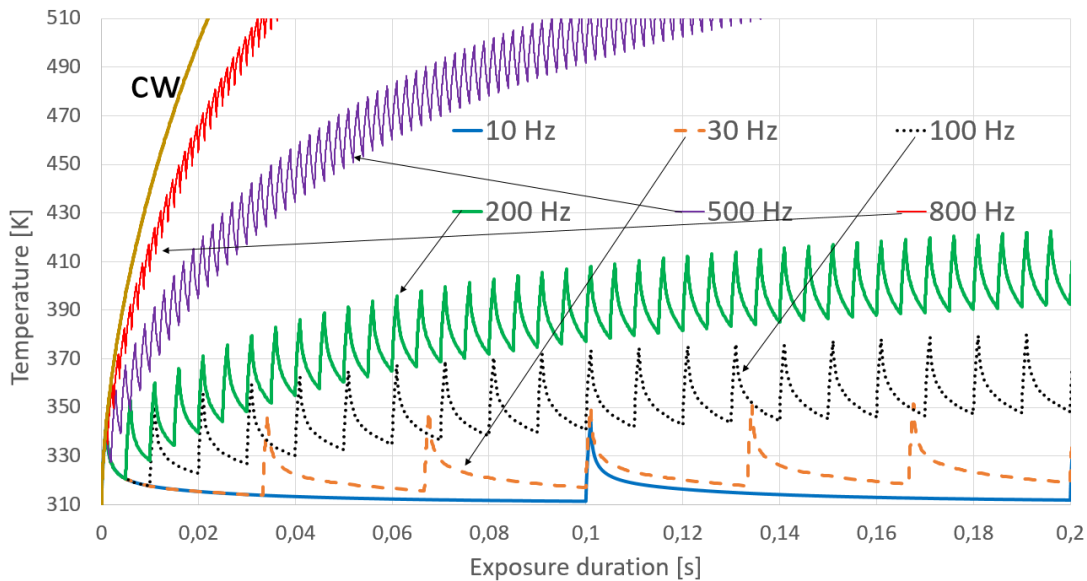


Figure 4. Time-temperature profiles calculated with the same energy per pulse for all pulse frequencies.

The higher the pulse frequency, the longer it takes for the background temperature increase to flatten out (to reach steady state), and the temperature increase on top of the background is then much smaller than the background temperature.

For the very small frequencies it is the background temperature increase above 310 K which is much smaller than compared to the temperature increase above background for each pulse.

Summary

Injury thresholds for a wavelength of 530 nm, pulse duration of 1 ms and $\alpha = 24$ mrad were used as example to discuss the dependence of the injury threshold on the number of pulses N.

The pulse repetition frequency was varied. High pulse repetition frequencies are adequately addressed by the average power requirement (Criterion 2 in IEC 60825-1). However, for intermediate and low pulse frequencies, the injury thresholds plotted as average power are getting lower and approach the average power MPE, so that the safety margin is reduced and the average power MPE no longer “covers” these lower pulse frequencies.

For the parameter choice of 1 ms and $\alpha = 24$ mrad, when plotted as energy per pulse, we see that for frequencies of roughly 100 Hz and somewhat less, a reduction of the single pulse AEL is needed. For a frequency of 100 Hz, $N^{-0.25}$ is found to fit the injury threshold reduction as function of N very well. The lower the pulse frequency becomes, the less pronounced is the reduction of the thresholds. For these low frequencies, $C_5 = N^{-0.25}$ can be seen as somewhat over-restrictive.

It is important to note that the critical frequency of 100 Hz - the frequency where $C_5 = N^{-0.25}$ describes the reduction of thresholds well - was found for the specific example of 1 ms pulse duration and $\alpha = 24$ mrad. Our database of thresholds shows that the critical frequency depends strongly on the pulse duration, but also, for α above α_{\max} , on the angular subtense of the apparent source α (i.e. on retinal image diameter).

The respective data will be presented and discussed in a peer review paper (to be submitted).

There is always a potential to improve the analysis rules for multiple pulses, where “improve” means that the analysis rules follow the injury thresholds ideally with a constant reduction factor as function of wavelength, pulse duration, pulse frequency, number of pulses, for various retinal image diameters (i.e. a 5-dimensional parameter space, even for regular pulse trains!). It is evident that any kind of change of the rules and limits would have to be done based on comprehensive analysis of a large collection of injury threshold data. Changes have to be done with caution so as to neither lower the permitted emission needlessly compared to current rules (i.e. to avoid making them more restrictive), nor to increase the permitted emission into a regime where safety is no longer assured.

It seems practically impossible to achieve a *simplification* of safety rules for the kind of complex threshold trends, without making them, for a notable parameter regime, either needlessly restrictive and/or

too high and potentially unsafe. Simple limits and limits that accurately follow threshold dependencies, including for irregular pulse trains, seem to basically rule each other out.

References

- [1] IEC 60825-1 Ed. 3.0 (2014): Safety of laser products – Part 1: Equipment classification and requirements.
- [2] ANSI Z136.1 Safe Use of Lasers (2014) Laser Institute of America.
- [3] Schulmeister K. (2013), The upcoming new editions of IEC 60825-1 and ANSI Z136.1 – Examples on Impact for Classification and Exposure Limits; ILSC 2013 paper #C102.
- [4] Schulmeister K. (2016), The new edition of the international laser product safety standard IEC 60825-1, White Paper, Seibersdorf Labor GmbH.
- [5] Schulmeister K. (2015), Analysis of pulsed emission under Edition 3 of IEC 60825-1; ILSC 2015 paper #202.
- [6] IEC 60825-1:2014/ISH1:2017, Interpretation sheet ISH1.
- [7] Jean M., Frederiksen A., Heussner N., Schulmeister K. (2019), Computer Modelling to Support Laser Safety Analysis of Pulse Trains with Varying Peak Power and Pulse Duration; ILSC conference proceedings, Orlando, USA; pages 66 – 72.
- [8] Jean M, Schulmeister K., Kotzur S., Frederiksen A. (2020), Validation of a generalized laser safety analysis method for irregular pulse trains, J Laser Appl 32, paper 032027.
- [9] Jean M. and Schulmeister K. (2017) Validation of a computer model to predict laser induced retinal injury thresholds, J Laser Appl. 029, 032004.
- [10] Schulmeister K., Sliney D.H., Stuck B.E. (2018), Comments on the application of the ICNIRP laser exposure limits, in: Proceedings of NIR 2018 Dresden, TÜV Media GmbH, Köln; p 321 - 345.
- [11] Schulmeister K. and Jean M. (2011), Manifestations of the Strong Non-Linearity of Thermal Injury, ILSC 2011 conference proceedings paper #901, p. 201-204.

Almost all the publications of the Seibersdorf Laboratories team can be downloaded from:

<https://laser-led-lamp-safety.seibersdorf-laboratories.at/downloads>